Analysis of dynamical properties
of object tracking system elements

Z. KUŚ*

Silesian University of Technology, Institute of Automatic Control, 16 Akademicka St., Gliwice, Poland

Abstract. The goal of this paper was to determine necessary dynamical conditions for the object tracking task. Developing these conditions required examining dynamical relationships between the UAV, camera head, disturbances and tracked object. This analysis was conducted in order to assess whether a given UAV-camera head set was suitable for a given object tracking task. The study assumed that the UAV was equipped with a flight trajectory control system. We discussed the methods of the dynamical properties description and finding a range of application for a particular set "UAV-camera head". For each dynamical element of the examined system, we proposed a method of computing the parameters of the simulation model which corresponded to the behaviour of the real elements. In order to describe the range of the applications for the UAV-camera head set, we defined the space Ω – all combinations of the parameters which characterized the dynamics of the disturbance and object. Moreover, this study developed the method of selecting the subspace Ω_s which described acceptable parameters of the object's and disturbance's dynamics. This paper presented the example of proper object tracking in the case of meeting the dynamical conditions and the example of losing the object in the opposite case.

Key words: unmanned aerial vehicles, object tracking, control system, dynamical model.

1. Introduction

The following paper is a part of research dedicated to the use of UAV equipped with a camera for observing terrestrial objects. Interestingly, the quick development of research in this field has resulted in new applications and solutions.

Just to name a few, we can enumerate the following applications: tracking moving objects [5], the surveillance of the area [8], vehicles moving on the roads [9] and, finally, searching for objects.

Furthermore, the directions of development can be divided into two major currents.

The first one focuses on the processing and analysis of the image obtained from a camera. This image is used for controlling on the upper levels of the control system (searching – object detection [7], object recognition [7], the calculation of the object position, object tracking [6] the calculation of the flight trajectory, automatic UAV's take-off and landing [3], the calculation of the UAV's position [1]. The second current focuses on developing the UAV's flight trajectory control alghoritms (take-off, no-collision flight and landing [3]), [4] for a specific type of the UAV, camera and camera head [10] taking into account the structure and the statical and dynamical properties of given equipment [2]. What is more, we can find the works which gather research on the use of the image from the mounted camera to control the UAV [11–13].

Owing to the intensive development of this research area, choosing an appropriate UAV-camera head set for a given tracking task may be a challenging task for the academic and in-

dustrial fields. It is interesting because the range of the use of tracking by means of a UAV has been growing both in the military and civil areas over the past few years.

On the one hand, the constantly growing use of applications results in greater and diverse requirements for a camera equipped UAV. On the other hand, the greater development of technical abilities of UAVs, camera heads and cameras increases the possibility of choosing the UAV-camera head set which is better suited for a given task, e.g. tracking, supervision or supporting other civil or military activities.

Therefore, it is of utmost importance to establish the criteria and methods of the equipment selection for the tasks which are to be done. The criteria may take into consideration various requirements such as: the flying range of the UAV, the ability to work not being noticed by a tracked object or to work in difficult atmospherical conditions, the cost of operation, the ability to store the data collected during the flight or other criteria.

We will focus on adjusting the possessed equipment to a task which must be carried out. The only criteria which we are going to take into account, are dynamical properties.

Hence the goal of the paper will be to determine the dynamical properties of the task (the dynamics of disturbance and a tracked object) which may be correctly carried out by a given UAV-camera head set.

This goal will be achieved in two steps. Firstly, we will present the method which will allow to model dynamical properties of a UAV, camera head, disturbances and a tracked object in the scope indispensable for a given task. Secondly, we will put forward the method of describing the dynamical properties of the tracking task on account of the dynamical properties of the tracked object and disturbance.

*e-mail: zkus@interia.pl

Finally, we will present the method of obtaining experimentally the range of dynamical properties of the object and disturbance for which a given UAV-camera head set will operate properly.

The developed algorithms should allow to select a simple and cheapUAV-camera head set which at the same time allows to track the object properly.

Therefore the dynamical models should accept basic assumptions: the simplicity of the parameters identification, describing only the dynamical properties which are of our interest and easy physical interpretation of the model's parameters. Finally, the obtained area of the possible applications of a given equipment should be determined by the parameters which are possible to determine for a given tracked object as well as working conditions.

2. The dynamical models of the UAV, camera head and disturbance

Taking into account that the core of this paper is to find the dynamical conditions of properly operating control system, the dynamical models of the elements of the examined control system will be proposed in the following section.

Therefore there will be two types of interactions between the UAV and environment which are going to be taken into account in the model of the UAV. Firstly, we will model the dynamics of following the set flight trajectory. Selecting the parmeters of the model, which guarantee the behaviour of the model similar to the behaviour of the real UAV, will be proposed in this paper. Secondly, we will ponder on the way of modelling the influence of disturbances on the UAV's orientation and location. Modelling the dynamics of the influence of disturbance on the UAV is carried out taking into account disturbances in the form of athmospherical phenomena such as rapid gusts of wind, heavy rain or local descending and ascending airstreams.

We assume that the UAV's change of location and orientation due to disturbances may be far more faster than restoring the UAV's location and orientation to correct values – values resulting from the set flight trajectory – after disturbance stops.

It is necessary to develop a multivariable model for the purposes of the synthesis of the flight trajectory control system. We assume the signals defining location (x_h, y_h, z_h) and rotation angles (α_h, β_h) of the UAV as the outputs of the model. The coupling channels will be skipped because of the assumption that the efficient flight trajectory control system was utilised (the decoupling of the multivariable system).

Therefore we will be assuming that it is possible to control each output not influencing remaining outputs.

Thus, the method of developing both models: the model of the dynamics of the UAV and the model of the influence of the disturbance on the UAV, will be presented herein for the one-variable case by means of using general variables.

For the multivariable case, the flight trajectory parameters are described by means of the multidimensional signal **y**. In the description of the multivariable case, the symbol y will denote a single output of the controlled plant. The

aforementioned output y corresponds subsequently to each element of the signal **y**. The elements of the vector signal **y** are as follows: x_h, y_h, z_h, – coordinates of UAV's location, α_h, β_h – UAV's rotation angles. Each output signal is connected with a corresponding set point signal and disturbance signal. Therefore the output, set point and disturbances signals are defined as shown in [1].

$$\mathbf{y} = \begin{bmatrix} x_h \\ y_h \\ z_h \\ \alpha_h \\ \beta_h \end{bmatrix} \quad \mathbf{y_{set}} = \begin{bmatrix} x_{hset} \\ y_{hset} \\ z_{hset} \\ \alpha_{hset} \\ \beta_{hset} \end{bmatrix} \quad \mathbf{z} = \begin{bmatrix} z_x \\ z_y \\ z_z \\ z_\alpha \\ z_\beta \end{bmatrix} \quad (1)$$

The lack of the coupling channels allows to analyse each single control loop as a separate control loop.

Considering a single close loop we can use the model shown in Fig. 1. It is simple model, yet it meets the abovementioned requirements. It is possible when the results shown in [14, 15] and trajectory control systems are taken into account. Hence the first order lag, intergrator and feedback loop provide proper representation of the dynamical properties of the UAV.
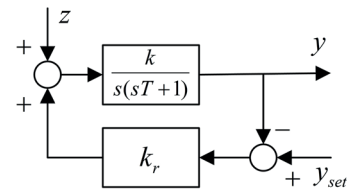

Fig. 1. The model of disturbances and set value effects on a controlled plant equipped with a control system

In order to analyse the operation of such a system we will use basics of control fundamentals [16]. The system which is presented in Fig. 1 is type I with respect to excitation $y_{set}(t)$. This means that the control system provides steady-state error $e(t)$ equal zero when the disturbance $z(t)$ is equal zero for $y_{set}(t) = y_{set0} \cdot \mathbf{1}(t)$. This, on the hand, means that the UAV's flight trajectory control system operates correctly.

The system is type 0 with respect to excitation $z(t)$. Therefore for the signal $z(t)$ with the constant and non-zero value, the control system is not able to guarantee the proper value of the signal y in a steady state. It is only after the disturbance stops when the value of the signal y returns to the set point value $y_{set}(t)$.

2.1. The dynamics of the UAV. An analysis of the dynamics of the UAV will be conducted by examining how the signal $y(t)$ follows the set point signal $y_{set}(t)$. According to Fig. 1, it

corresponds to the movement of the UAV along the set point trajectory. On the basis of Fig. 1 it may be stated that the transfer function between $y_{set}(t)$ and $y(t)$ is described in (2).

$$\frac{Y(s)}{Y_{set}(s)} = \frac{kk_r}{s(sT+1)+kk_r} \tag{2}$$

The poles of this transfer function are defined by (3).

$$s_1 = -\frac{1}{2T} + \frac{\sqrt{1-4Tkk_r}}{2T}$$
$$s_2 = -\frac{1}{2T} - \frac{\sqrt{1-4Tkk_r}}{2T} \tag{3}$$

Time constants corresponding to these poles are presented in (4).

$$T_1 = \frac{2T}{1-\sqrt{1-4Tkk_r}} \qquad T_2 = \frac{2T}{1+\sqrt{1-4Tkk_r}} \tag{4}$$

Assuming that the poles s_1 and s_2 belong to real numbers we obtain time constants T_1 and T_2 which are real and positive. This condition is met for $4kk_rT < 1$. Time constant T_1 is greater than T_2 and T_1 decides about the speed of reaction of the UAV on controlling the flight trajectory. We can observe that the greater value of k_rk is, the lower T_1 is. At the same time, the lower T allows to achieve the lower T_1. Therefore, by means of increasing kk_r and decreasing T, we obtain faster dynamics of the UAV which corresponds to obtaining faster the set point value $y_{set}(t)$ by the signal $y(t)$. At the same time, we can observe that the maximum linear and angular velocities of the UAV, which decide about speed of shift and rotation of the UAV, are the significant dynamical parameters of the UAV model. For the model presented in Fig. 1 with assumptions that $y_{set}(t) = y_{set0} \cdot \mathbf{1}(t)$, we obtain the formula for the maximum speed of signal $y(t)$ changes, cf (5).

$$V_{ymax} = \frac{y_{set0}}{T_1 - T_2} \cdot \left(e^{\frac{T_2 \cdot \ln T_2/T_1}{T_1 - T_2}} - e^{\frac{T_1 \cdot \ln T_2/T_1}{T_1 - T_2}} \right) \tag{5}$$

2.2. The dynamics of disturbances. When we examine the dynamics of the influence of distrubances on a UAV, we can observe that the transfer function between the disturbance $z(t)$ and the output $y(t)$ is defined in (6).

$$\frac{Y(s)}{Z(s)} = \frac{k}{s(sT+1)+kk_r} \tag{6}$$

In the steady-state the signal $y(t)$ in response to the constant disturbance $z(t) = z1(t)$ obtains the value $y_u = z_o/k_r$. Hence the control system cannot in this case compensate the disturbance. What is more, for a small k_r the component of signal $y(t)$ dependent on disturbance $z(t)$ may be significantly high.

Our aim is to model independently the dynamics of the influence of disturbances and the set point signal on the UAV. At the same time, we can see that the poles of the transfer function (6) are the same as the poles of the transfer function (2). This fact causes that this independence is impossible to achieve by means of the close loop parameters: kk_r and T. However, there is a possibility of independent modelling of the disturbance influence on the UAV's behaviour by means of providing an appriopriate shape of the signal $z(t)$. We assume that $z(t)$ is a square signal with amplitude A_z and duration T_z. The greater A_z we have, the faster reaction of the UAV on disturbance we achieve. Furthermore, greater T_z causes the greater changes of UAV's location or rotation. In this way, we can model the disturbance influence on the UAV independently on the dynamics of the flight trajectory control system.

2.3. The dynamics of the camera head. The model of the camera head on the example of the control channel for the angle α is presented in Fig. 2. The transfer function which
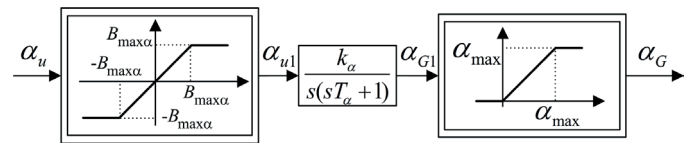

Fig. 2. The model of the dynamics of the camera head

defines the dynamics of the camera head is presented in the equation (7)

$$\frac{\alpha_{G1}(s)}{\alpha_{u1}(s)} = \frac{k_\alpha}{s(sT_\alpha+1)} = \frac{k_\alpha}{s} + \frac{-k_\alpha T_\alpha}{sT_\alpha+1} \tag{7}$$

What we can see in (7), there are two elements: an integrating element responsible for modelling the speed of the camera head rotation and first order lag element responsible for modelling the load of the engine by the weight of the camera. Increasing k_α corresponds to a greater speed of the camera head rotation while increasing T_α corresponds to greater inertia – the slower reaction of the camera head on the changes of the input signal α_{u1}. There are also two saturation blocks in the model. The input saturation block causes that the maximum speed of the camera head rotation is $V_{\alpha max} = k_\alpha \cdot B_{\alpha max}$. The output saturation block limits the angle of the camera head rotation in the vertical plane. It is connected with the limited usefulness of the images obtained when α_k is approaching 90 degrees. In this case the significant perspective distortions appear.

The model of the camera head for the control channel of the angle β is similar; however, it does not have any limit of the angle β value. Therefore the saturation in the output of the transfer function does not appear.

The dynamical models for the elements of the control system are presented above; however, in the next step it is necessary to define geometrical relationships between these elements.

3. The geometrical variables defining the location and orientation of the object tracking system's elements

The whole examined system consists of the UAV with the mounted camera head, tracked object or supervised surface, plane of the ground and various disturbances.

The method presented in the paper may be applied to any UAV, taking into account specific limitations. In this study, a helicopter was used as an example of a UAV.

Basic assumptions, which refer to geometrical relations for the examined problem, were elaborated in [17, 18].

We assume that:

d) the UAV's position equals camera position ($x_h = x_k$, $y_h = y_k$, $z_h = z_k$)

e) the camera orientation is a sum of UAV's orientation and camera head's rotation;

f) the tracked object moves on a flat earth ($z_o = 0$);

g) the camera head may rotate within the range of 360 degrees in horizontal plane – parallel to the bottom of the UAV and within the range of 90 degrees in a vertical plane.

Similarly, as it was presented in [18] the current object position is calculated only in the moment when pattern recognition algorithms give information that the object is in the camera field of view.

The UAV's orientation is described by two rotations angles: α_k (in the vertical plane) and β_h (in the horizontal plane).

Figures 3 and 4 present the scheme of the calculations for a case when the disturbance occurs. Figure 3 presents the pro-

jection on the horizontal plane for the example of the disturbance which acts when the camera is turned towards the object. The camera is turned correctly for $\beta_k = \beta_{k1}$ and the object is visible in the camera field of view in this case. The control system calculates $\beta_{kset} = \beta_{k1}$ and tracked object's location (x_o, y_o). Then the disturbance turns the camera to the angle β_{k2}; consequently, the tracked object is lost from the camera field of view. The rotation angle β_{krot} is calculated as $\beta_{krot} = \beta_{kset} - \beta_{k2}$. The rotation of the camera by the angle β_{krot} results in the object returning to the camera field of view. There are no changes of the location in this case. Figure 4 presents the scheme of the calculations for the case when the disturbance changes angle α_k. The camera is turned correctly for $\alpha_k = \alpha_{k1}$ and the object is visible in the field of view in this case. The control system calculates $\alpha_{kset} = \alpha_{k1}$ and tracked object's location (x_o, y_o). Then the disturbance turns the camera to the angle α_{k2} which results in losing the tracked object from the camera field of view. The rotation angle α_{krot} is calculated as $\alpha_{krot} = \alpha_{kset} - \alpha_{k2}$. The rotation of the camera by the angle α_{krot} results in returning the object to the camera field of view. There are no changes of the location in this case. Taking into consideration the control process from the UAV's take-off, we assume that in the first stage the UAV is being steered by an operator towards the object. When the object appears in the screen of the control panel, the operator marks it as an tracked object. In this way, the image processing block gets information about tracked object's look. Therefore we can state that when the control system starts, the tracked object is visible in the camera field of view. According to the points 1) and 2) in Fig. 3 and 4, it is possible
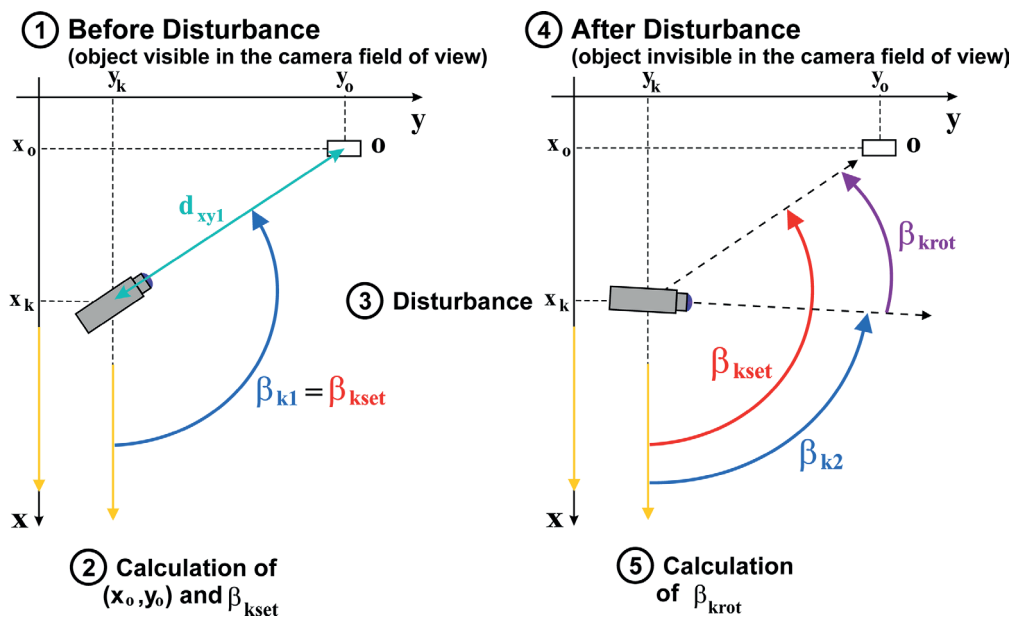

Fig. 3. The distances and angles for a projection on a horizontal plane and the order in which calculations are processed before and after the disturbance
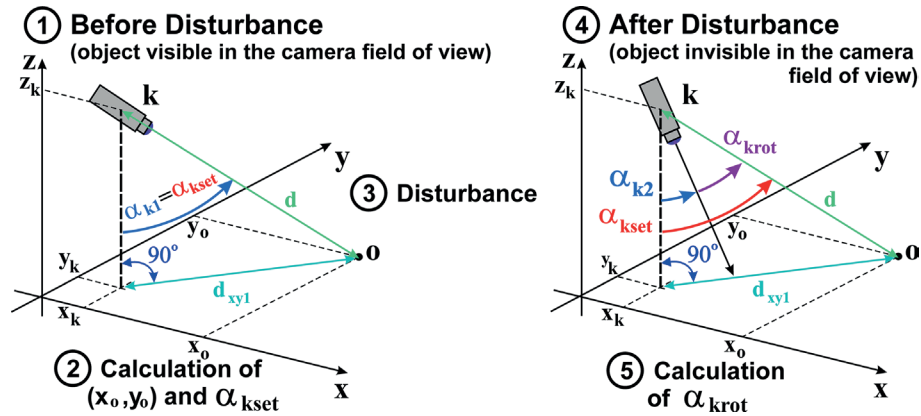
Fig. 4. The distances and angles for a projection on a vertical plane and the order in which calculations are processed before and after the disturbance

to calculate the object's location thanks to the fact that the camera is turned towards the object. The position of the object (x_o, y_o) is calculated on the basis of rangefinder data (distance d), GPS and IMU data $(x_k, y_k, z_k, \alpha_k, \beta_k)$ cf equation (8).

$$\left.\begin{array}{l} x_o = x_k + d_{xy1} \cdot \sin(90^o - \beta_k) \\ y_o = y_k + d_{xy1} \cdot \cos(90^o - \beta_k) \end{array}\right\} \text{ for } \beta_k \in \langle 0^o, 180^o \rangle$$

(8)

$$\left.\begin{array}{l} x_o = x_k + d_{xy1} \cdot \sin(90^o + \beta_k) \\ y_o = y_k - d_{xy1} \cdot \cos(90^o + \beta_k) \end{array}\right\} \text{ for } \beta_k \in \langle -180^o, 0^o \rangle$$

where $\quad d_{xy1} = z_k \cdot \tan(\alpha_k)$

We assume that the object is in the center of the picture during measurements. It causes that we assume the values α_k and β_k as the set point values α_{kset} and β_{kset}. According to the point 3 in Fig. 3 and 4, there is disturbance and in the point 4, after disturbance, the camera is not directed towards the tracked object. Figures 3 and 4 shows the examples in which disturbance changes only the angles α_k and β_k. For the case when the angles and positon of the camera are changed simultaneously by disturbance, the calculations are made in the same way. Next, the control system calculates the direction in which the camera has to be turned in order to be turned towards the tracked object again. For the case presented in Fig. 3 and 4, without the shift of the camera, after disturbance the required rotation angle is the same as the angle calculated in the point 2 and d_{xy2} (d_{xy} after disturbance) is equal d_{xy1} (d_{xy} before disturbance). In a general case, assuming that disturbance influences both the change of orientation and the location of the camera, we calculate the set point values of the angles α_k and β_k on the basis of location and orientation of the camera and previously calculated object's location. The respective equations for calculating α_{kset} and β_{kset} are presented in (9).

$$\alpha_{kset} = \arctan\left(\frac{d_{xy2}}{z_k}\right)$$

where $\quad d_{xy2} = \sqrt{(x_k - x_o)^2 + (y_k - y_o)^2}$

(9)

$$\beta_{kset} = -90^o - \arctan\left(\frac{x_o - x_k}{y_o - y_k}\right) \quad \text{for} \quad y_k \geq y_o$$

$$\beta_{kset} = -90^o - \arctan\left(\frac{x_o - x_k}{y_o - y_k}\right) \quad \text{for} \quad y_k \geq y_o$$

In the next step we will calculate the correction angles α_{krot} and β_{krot} at which we have to turn the camera in order to direct the camera towards the object. The calculations are conducted according to (10).

$$\alpha_{krot} = \alpha_{kset} - \alpha_k; \qquad \beta_{krot} = \beta_{kset} - \beta_k \qquad (10)$$

It corresponds to the point 5 for the case shown in Fig. 3 and 4. Afterwards, the camera turns towards the object and we can use: the image processing block and the location of the object in the picture, to control the camera head.

Using the dynamical and geometrical properties of the control system's elements, in the next section we will develop the control system.

4. The control system and the analysis of the dynamical properties of its elements

The dynamical model of the examined control system will be proposed in the following section. The basic parts of such a system are: UAV's flight trajectory control system and camera head control system.

4.1. The UAV's flight trajectory control system. In the section 2 of the following paper we discussed the UAV's flight trajectory control system. According to Fig. 1, the variables k,

kr and T define the dynamics of the UAV. We should select these parameters in such a way that the behaviour of the UAV's model corresponds the real UAV's behaviour. If we bear in mind that the greater kkr and lower T we have, the faster we reach the set point value, than we can select the appropriate values of these parameters. Owing to the fact that an integrator is a part of the model, the output signal reaches the set point value when there are not any disturbances. The variables T_1 and k decide about the speed of the changes of the signal y. Figure 5 presents the control system for the UAV and camera head for the control channel of the angle α_k.
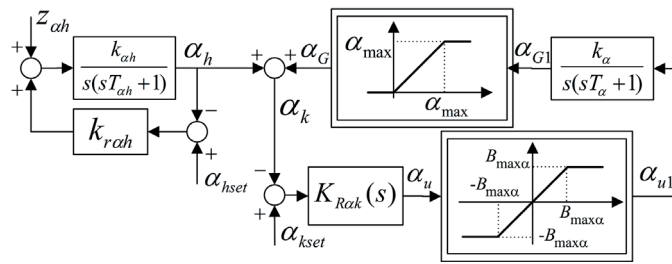

Fig. 5. The UAV's and camera head's control systems for the control channel of the angle α_k

4.2. The camera head control system. According to Fig. 5, it is necessary to select in the control system the values of k_α, T_α, α_{max} and $B_{max\alpha}$. These values have to guarantee that the velocities and ranges of α_k and β_k do not exceed maximum values characteristic for a given type of a camera head.

In order to examine the dynamics of the camera head, we skip saturation blocks in Fig. 5 and then the transfer function between α_{kset} and α_k may be described as (11).

$$\frac{\alpha_k(s)}{\alpha_{kset}(s)} = \frac{k_\alpha k_{r\alpha k}}{s(sT_\alpha + 1) + k_\alpha k_{r\alpha k}} \qquad (11)$$

The time constants of this transfer function are presented in (12).

$$T_{1\alpha} = \frac{2T_\alpha}{1 - \sqrt{1 - 4T_\alpha k_\alpha k_{r\alpha k}}};$$
$$T_{2\alpha} = \frac{2T_\alpha}{1 + \sqrt{1 - 4T_\alpha k_\alpha k_{r\alpha k}}}; \qquad (12)$$

We assume that $T_{1\alpha}$ and $T_{2\alpha}$ belong to the real numbers. Additionally, for $4T_\alpha k_\alpha k_{r\alpha k} = 1$ we obtain $T_{1\alpha} = T_{2\alpha} = 2T_\alpha$ and these time constants decide about the dynamics of the camera head. The abovementioned analyses were conducted assuming that the P regulator was used.

The model for the control channel of the angle β is similar.

4.3. Finding the application range for a given set 'UAV – camera head'. It seems to be valuable for a practical application to elaborate the algorithm for the following task: we have

a particular type of the UAV and the camera head and we have to determine the range of use for the abovementioned equipment. This range of use is defined by the dynamics of both: the object and disturbances for which object tracking is possible.

The algorithm of finding the application range for a given set 'UAV – camera head' is presented as follows:

A. We identify the real UAV's parameters by means of conducting an experiment to find the step response of the UAV in each control channel.

B. We select k, k_r and T in the UAV's model (for each control channel) so as to obtain the simulation transients similar to transients obtained during the real UAV's flight. It means that the conditions from (13) have to be met.

$$T_1 = T_h; \qquad V_{ymax} = V_{hmax}; \qquad 4kk_rT < 1 \qquad (13)$$

The sequence of the calculations which guarantee meeting the conditions (13) is following:

B1. We assume that $T_1 = T_h$ and consequently we have the equation $T_1(k, k_r, T) = T_h$;

B2. We assume y_{set0} as a maximum value of the predicted step of the set point value;

B3. From the formula which allows to calculate $V_{ymax} = V_{ymax}$ (y_{set0}, T_1, T_2) we compute T_2 for previously assumed T_1 and y_{set0} and we denote computed T_2 value as T_{2max}. Hence we obtain the equation $T_2(k, k_r, T) = T_{2max}$. In this way, we can present the conditions (13) as (14).

$$\frac{2T}{1 - \sqrt{1 - 4Tkk_r}} = T_h; \quad \frac{2T}{1 + \sqrt{1 - 4Tkk_r}} = T_{2max}; \quad kk_rT < 0.25; \quad (14)$$

By calculating the values of the variables k, k_r and T which meet the coditions (14), we find the UAV's model corresponding a particular type of the UAV.

C. We conduct an analogical experiment, with the step response, for the camera head. It allows to obtain the time constants $T_G(T_{G\alpha}, T_{G\beta})$ and the maximum rotation velocities $V_{Gmax}(V_{G\alpha max}, V_{G\beta max})$ of the real camera head.

D. The conditions from (15) have to be met if we want to obtain the equivalent dynamical properties of the model and real camera head.

$$T_{1\alpha} = T_{2\alpha} = 2T_\alpha = T_{G\alpha};$$
$$V_{G\alpha max} = V_{\alpha max} = k_\alpha \cdot B_{\alpha max} \qquad (15)$$
$$4T_\alpha k_\alpha k_{r\alpha k} = 1$$

The sequence of calculations is following:

D1. We calculate $T_\alpha = T_{G\alpha}/2$;

D2. We assume that the gain of the P regulator should be far greater than the gain of the plant – so that the steady-state error in response to disturbance in the input is minor. Therefore we assume $k_{r\alpha k} = m \cdot k_\alpha$ where $m \gg 1$;

D3. We calculate the gain of the plant $k_\alpha = \sqrt{\frac{1}{2 \cdot m \cdot T_{G\alpha}}}$ and for the calculated k_α we compute $B_{max\alpha} = \frac{V_{G\alpha max}}{k_\alpha}$;

In this way, we calculate the parameters of the camera head model.

E. We introduce the space $\Omega = (T_z, A_z, V_o)$. Each point of this space defines the values of the dynamical parameters for the object and disturbance. Our goal is to find the subspace Ω_s containing the values of parameters T_z, A_z and V_o which allow to track the object without losing it. Obviously, $\Omega_s \in \Omega$. In order to define Ω_s, we have to find the maximum value of the object velocity V_{omax} which allows to track the object without losing it. It is conducted for each pair (T_z, A_z). $V_{omax}(T_z, A_z)$ is the maximum acceptable value of V_o – the maximum value of V_o for which tracking is conducted without losing the object. $V_{omax}(0, 0)$ is the maximum acceptable value of V_o when there are not any disturbances.

F. Therefore we assume the test trajectory of the object (fig. 6) which is designed in such a way that its shape hinders object tracking as much as possible. We obtain the disturbance always in the same places on the object's trajectory, however, the time between the appearance of subsequent disturbances is getting shorter for the greater values of V_o.
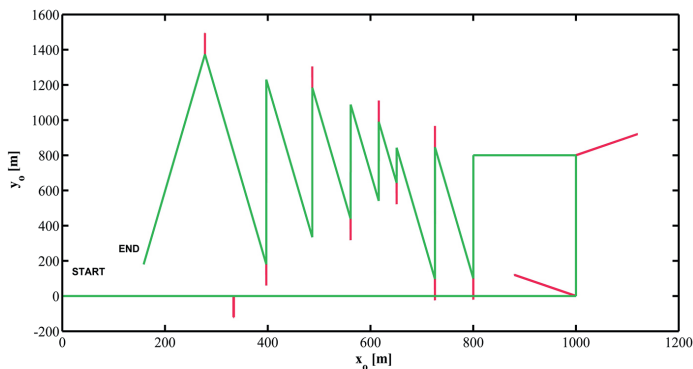

Fig. 6. The test trajectory of the object with denoted (red line) directions of the disturbances

During the experiments we used two disturbance channels: the shift of the UAV in the plane (x, y) and the change of the angle β_h. These disturbance channels were chosen as highly-influencing the tracking process. The both disturbances always co-occur. The directions of the disturbances which shift the UAV in the plane (x, y) (fig. 6) were selected in such a manner that the UAV was being moved away from the object as much as possible.

We find V_{omax} for a given point in the plane V_{omax} in the following manner:

We conduct an object tracking experiment (for the test trajectory shown in Fig. 6) for the velocity V_o which increases in each experiment. V_o is increasing between the experiments so long as to obtain the value of V_o for which the object is lost. We assume the greatest value of V_o, for which the object is not lost, as V_{omax} for a given point (T_z, A_z).

G. In this way, we obtain the subspace Ω_s which defines in the space Ω a set of dynamical parameters which allow to track the object. For a particular type of the UAV we can interpret

the A_z as the metricated power of the wind; moreover, we can interpret T_z as the duration of the gust of wind.

The presented method may be used to conduct the experiments better suited to particular applications. For example, the test trajectory may be suited to a predicted type of tracked object and terrain where the object will move. The number of the conducted experiments and density of the tested disturbance parameters may be suited to the dynamical properties of the examined system.

5. The examples illustrating the necessity of fulfilling the dynamical conditions of the object tracking

In this section, we will present the examples of the object tracking. The first example will present a situation in which the dynamics of the UAV and camera head is fast enough in respect to the object dynamics. In this case, the dynamical conditions are met and object tracking is carried out successfully. The second example will present a situation in which the dynamical conditions are not met (the dynamics of the object is too fast in respect to the dynamics of the UAV and camera head).

In the following example we will use the particular type of the UAV: helicopter Vario XLV presented in Fig. 7 and examined in [19].

Fig. 7. The helicopter Vario XLV [19]

The camera head which we will examine is the gimbal camera head described in [19, 20].

Fig. 8. The gimbal camera head with the video and thermovision camera [19]

On the basis of the examination of the helicopter Vario XLV dynamics, we assumed the values of the parameters T_h and V_{hmax}, for the subsequent control channels, which are presented in Table 1. The parameters which characterise the

Table 1
The values of the parameters T_z and V_{hmax} for the UAV's control channels

UAV	x_h	y_h	z_h	α_h	β_h
T_h	5 [s]	5 [s]	2 [s]	1 [s]	1 [s]
V_{hmax}	80 [km/h]	80 [km/h]	40 [km/h]	60 [º/s]	60 [º/s]

Table 2
The values of the parameters T_G and V_{Gmax} for the control channels of the angles α_k and β_k

Camera head	α_k	β_k
T_G	0.1 [s]	0.1 [s]
V_{Gmax}	250 [º/s]	250 [º/s]

dynamical properties of the camera head were assumed on the basis of the transients and data taken from [19, 20] and these are respectively: $T_G = 0.1[s]$ and $V_{Gmax} = 250[o/s]$. The helicopter's and UAV's parameters are presented in the tables 1 and 2. Tables 3 and 4 present the calculated parameters of the camera head's and UAV's models.

Table 3
The values of the UAV's model parameters for subsequential control channels

UAV	x_h	y_h	z_h	α_h	β_h
k	0.38	0.38	0.6	0.85	0.85
k_r	0.38	0.38	0.6	0.85	0.85
$T[s]$	1.38	1.38	0.55	0.28	0.28

Table 4
The values of the camera head's model parameters for the control channels of the angles α_k and β_k

Camera head	k_α / k_β	$k_{r\alpha k} / k_{r\beta k}$	T_α / T_β	B_{max}	α_{max}
α_k	0.7	7	0.05 [s]	353	75 [º]
β_k	0.7	7	0.05 [s]	353	-

Next, according to the description from section 4, we carry out the simulations which allow to find the size of the subspace Ω_s. For the examined helicopter and camera head we obtain the subspace Ω_s presented in Fig. 9. In Fig. 9 we have chosen green rings to denote the points of the space Ω for which the object

is not lost during tracking. The red rings denote the points for which the tracked object is lost during tracking. According to Fig. 9, increasing T_z and A_z results in decreasing the acceptable value V_o. In order to assess the usefulness of the obtained subspace Ω_s, we will conduct test simulations. We will choose two sets of parameters (T_z, A_z, V_o).
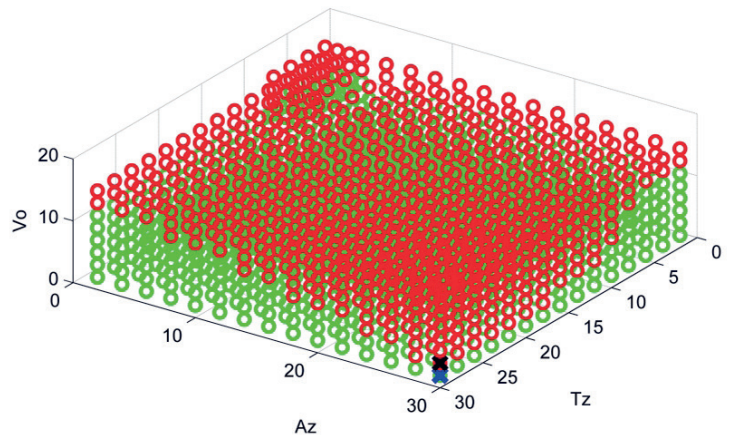

Fig. 9. The subspace Ω_s. Blue x – test point number 1, black x – test point number 2

Figure 9 presents the two kinds of test points of the space Ω: belonging and not belonging to the subspace Ω_s.

Experiment 1. $(V_o = 2, \; T_z = 30, \; A_z = 30)$

During the experiment 1 we assume the dynamical parameters of the object and disturbance in the space Ω which correspond to the point number 1 from Fig. 9. Test point number 1 is inside Ω_s.

Figure 10 presents two trajectories. The red numbers denote the tracked object trajcectory and the green numbers denote the point on the gound which is seen in the center of the image. According to the Fig. 10, the disturbances cause small shifts of the red and green line after the disturbance.

Figure 11 presents the UAV's and object's trajectories in the plane (x, y). We see in the Fig. 11 that the UAV's trajectory is strongly distorted during disturbance.

Figure 12 presents the transients of $x_h, x_o, z_{xh}, y_h, y_o, z_{yh}, u_1$, and u_2 for the test point number 1. u_1 is equal 1 when the object is out of the camera field of view. u_2 is equal 1 when the control system loses object. The signal u_2 in all figures is shifted up to make the figure clear. The value of the singal u_2 equal 0 corresponds to the value equal 0,5 in the figure and the value of the singal u_2 equal 1 corresponds to the value equal 1,5 in the figure. In Fig. 12, we can clearly observe the moments of changes of the camera's location and orientation during disturbances. Moreover, we can see that the object is not lost from the camera field of view for any time. The signal u_2 is equal 0 during all simulation of object tracking which means that the object is not lost. This is the case which we expected because the test point number 1 is inside the subspace Ω_s.
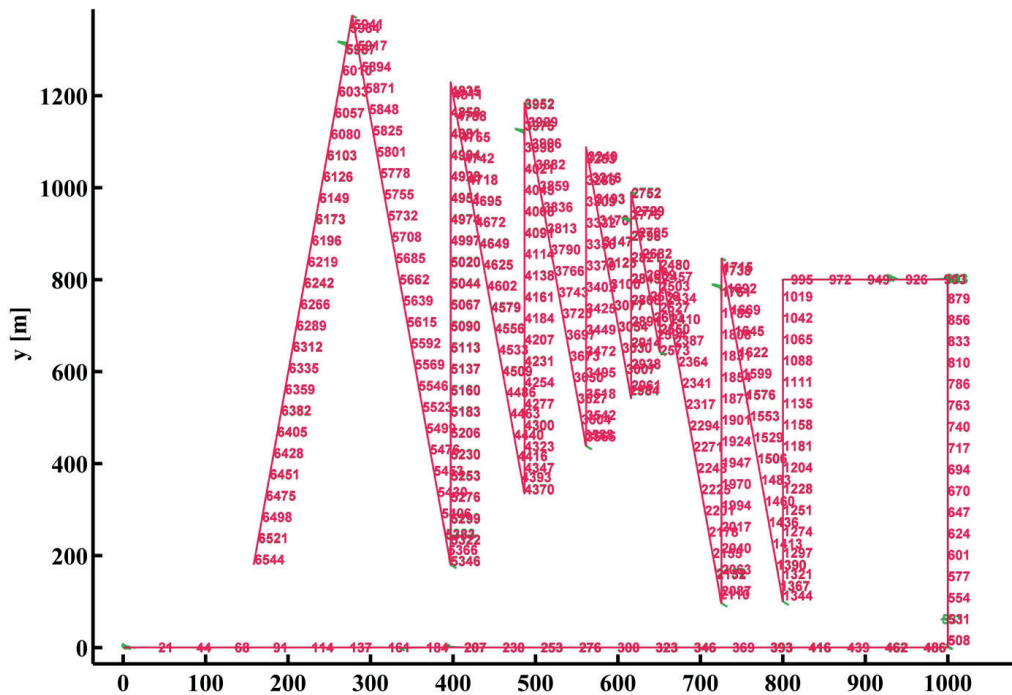
Fig. 10. The object trajectory and the trajectory of the point visible in the centre of the camera field of view for a test point number 1
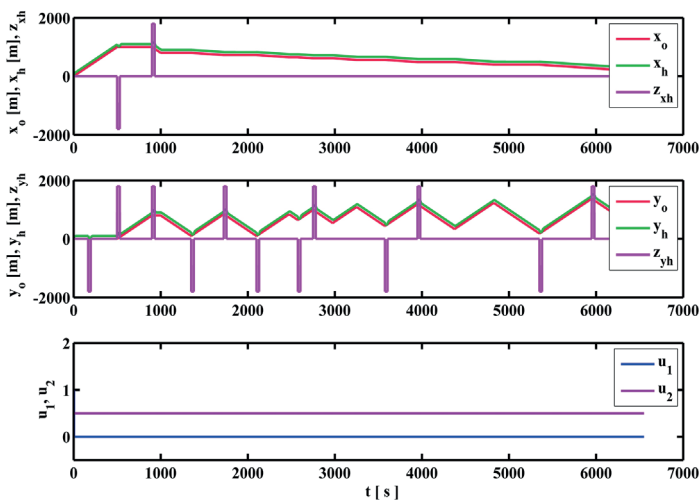

Fig. 12. The transients of x_h, x_o, z_{xh}, y_h, y_o, z_{yh}, u_1, and u_2 for the test point number 1
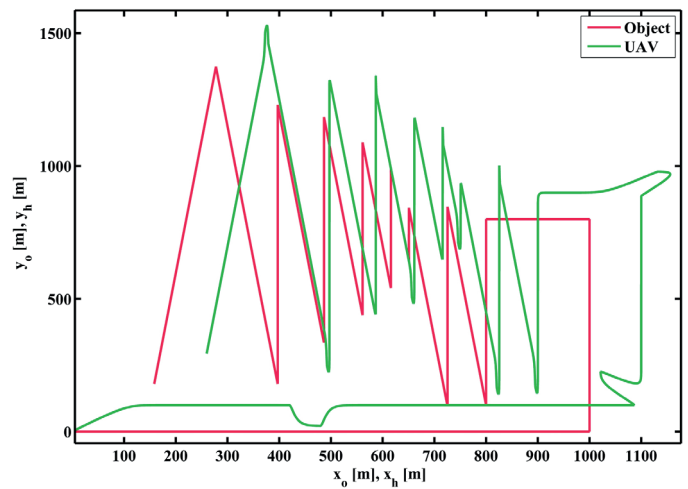

Fig. 11. The object's and UAV's trajectories for a test point number 1

Experiment 2.   ($V_o = 4$, $T_z = 30$, $A_z = 30$)

During the experiment 2 we assume the dynamical parameters of the object and disturbance in the space Ω which correspond to the point number 2 from the Fig. 9.

Figure 13 presents the object trajectory and the trajectory of the point visible in the centre of the camera field of view for the test point number 2.

We can clearly see in fig. 13 that the there are great distortions of the green line after the disturbances.

The UAV's and object's trajectories in this case, for the test point number 2, are similar to the trajectories presented in fig. 11.

Figure 14 presents the transients of x_h, x_o, z_{xh}, y_h, y_o, z_{yh}, u_1, and u_2 for the test point number 2. When the value of the signal u_2 equal 1 appears in the five moments, it means that the control system loses the object in these very moments.

In this case, we can see that there is a momentary loss of the object from the camera field of view and the control system loses the object. This is the result which we expected because the test point number 2 is from the outside of the subspace Ω_s.
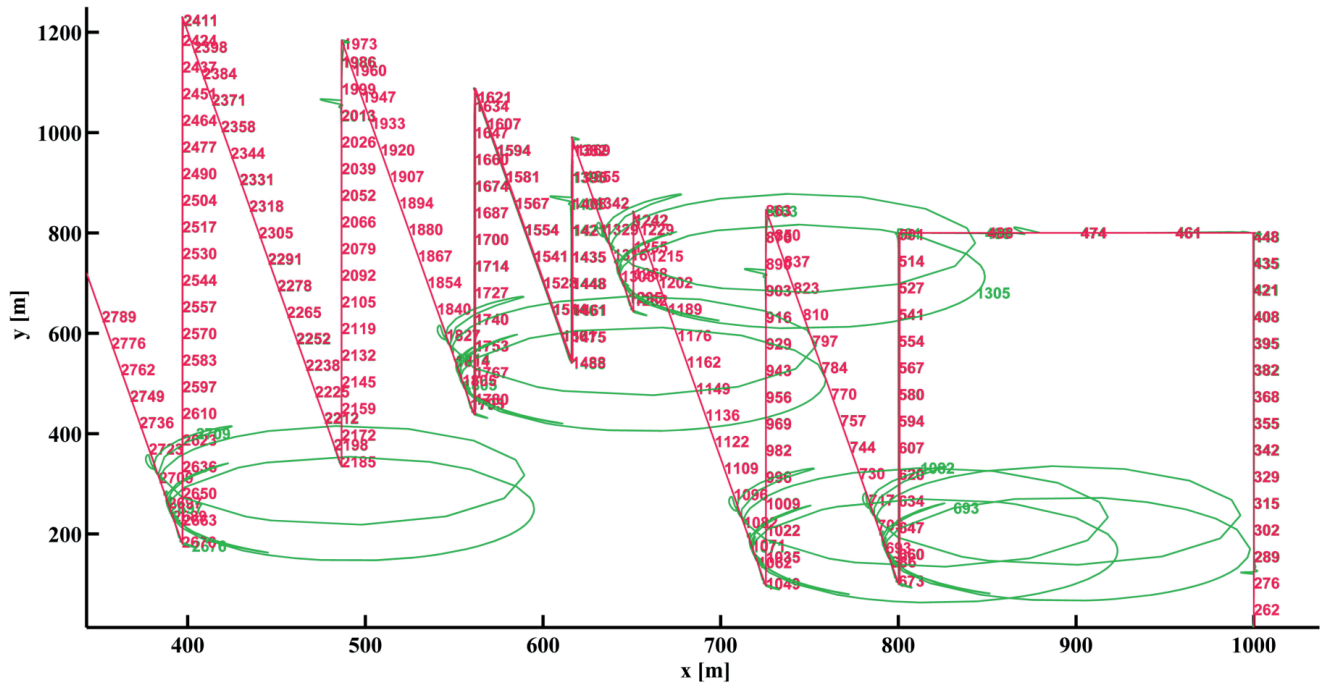
Fig. 13. The object trajectory and the trajectory of the point visible in the centre of the camera field of view for the test point number 2
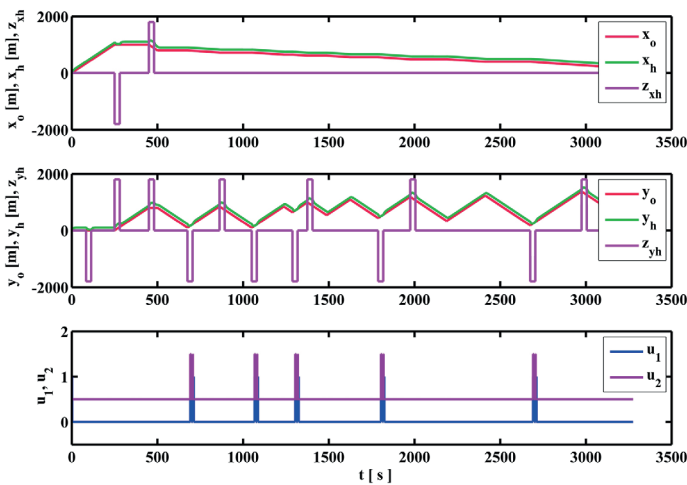

Fig. 14. The transients of x_h, x_o, z_{xh}, y_h, y_o, z_{yh}, u_1, and u_2 and u_2 for the test point number 2

6. Conclusions

The presented paper has elaborated on completing the UAV-camera head set for the realisation of the particular object tracking task. The proposed method was based on the dynamics of the elements involved in object tracking with the use of the UAV.

The presented solution of such a formulated task consists of two main elements: A) the method of the dynamical properties description and B) the method of finding a range of application for a particular UAV-camera head set.

In order to solve the first stage (element A), we proposed a simple though useful model of the dynamics of the UAV, camera head, object and disturbances. It was assumed during UAV modelling that the UAV is equipped with a flight trajectory control system and, in this way, we could focus on the very dynamics of the flight trajectory control system.

Likewise the camera head's model accounts basic dynamical parameters such as the speed of reaction and maximum angular velocity. To describe the dynamics of the tracked object, we concentrated on the following parameters: maximum velocity with which the object is able to move on the earth and the shape of the trajectory of the object movement. For each dynamical element of the examined system, we proposed a method of calculating the model's parameters in such a way that they corresponded to the behaviour of the real elements (UAV, object, disturbance and camera head). Solving the second stage (element B) involved a description of the range of the applications for the UAV-camera head set in the form of the subspace $\Omega_s \in \Omega = (T_z, A_z, V_o)$, where Ω is the space of all combinations of the parameters which characterize the dynamics of the disturbance and object.

The developed method of determining Ω_s required to make certain assumptions (e.g. the shape of the trajectory of the object movement, the moments when the disturbance starts). However, the possibility of modifying these assumptions, namely the conditions of the experiment, allowed to adjust the experiments to the particular application of the set UAV-camera head in the object tracking task. Moreover, the paper presented an example illustrating how the developed algorithms operate and this example showed that finding Ω_s may be useful for assessing

whether a given UAV-camera head set is suitable for a particular object tracking task.

References

[1] I.F. Mondragon, P. Campoy, C. Martinez, and M.A. Olivares-Mendez, "3D pose estimation based on planar object tracking for UAVs control", *IEEE International Conference on Robotics and Automation (ICRA)* (2010).

[2] F. Ivan, Mondragon, A. M. Olivares-Mendez, P. Campoy, C. Martinez, and L. Mejias, "Unmanned aerial vehicles UAVs attitude, height, motion estimation and control using visual systems", *Autonomous Robots* 29(1), 17–34, (July 2010).

[3] K. E. Wenzel, A. Masselli, and A. Zell, "Tracking and Landing of a Miniature UAV on a Moving Carrier Vehicle", *Journal of Intelligent & Robotic Systems* 61, 221–238 (2011).

[4] B. Jung and G.S. Sukhatme, "Real-time motion tracking from a mobile robot", *International Journal of Social Robotics* 2(1), 63–78 (2010).

[5] Y. Lin, Q. Yu, G. Medioni, "Efficient detection and tracking of moving objects in geo-coordinates", *Machine Vision and Alications* 22(3), 505–520 (2011).

[6] H. Mao, Ch. Yang, G. P. Abousleman, J. Si, "Automated multiple target detection and tracking in UAV videos", *Proc. SPIE 7668, Airborne Intelligence, Surveillance, Reconnaissance (ISR) Systems and Alications VII*, 76680J, (2010).

[7] S. Wu, O. Oreifej, M. Shah, "Action recognition in videos acquired by a moving camera using motion decomposition of Lagrangian particle trajectories", *Proceedings of the 2011 International Conference on Computer Vision* (2011).

[8] Z.H. Khan, I.Y.-H. Gu, "Joint feature correspondences and aearance similarity for robust visual object tracking, information forensics and security", *IEEE Transactions* 5(3) (2010).

[9] J. H. Choi, D. Lee, H. Bang, "Tracking an unknown moving target from UAV extracting and localizing a moving target with vision sensor based on optical flow", *5th International Conference on Automation, Robotics and Alications* (2011).

[10] J. Kim, D. Lee , K. Cho, S. Jo, J. Kim, C. Min, D. Han, S. Cho, "Development of an electro-optical system for small UAV", *Aerospace Science and Technology*, 14(7) (2010).

[11] P. Kimon, R. Beard, P. Oh, A. Ollero, L.A. Piegl, H. Shim, *Selected Papers from the 2nd International Symposium on UAVs*, Reno, Springer, 2009.

[12] B. Bhanu, C.V. Ravishankar, A.K. Roy-Chowdhury, H. Aghajan, D. Terzopoulos, *Distributed Video Sensor Networks*, Springer, 2011.

[13] J. Luo, "Affective computing and intelligent interaction", *Advances in Intelligent and Soft Computing* 137 (2012).

[14] Z. Kuś, S. Fraś, "Helicopter control algorithms from the set orientation to the set geographical Location", *Studies in Computational Intelligence* 440 (2013).

[15] A. Nawrat, *Modelowanie i sterowanie bezzałogowych obiektów latających*, Wydawnictwo Politechniki Śląskiej, Gliwice, 2009.

[16] R. Gessing, *Control Fundamentals*, Silesian University of Technology, Gliwice, 2004.

[17] Z. Kuś, A. Nawrat, "Object tracking in a picture during rapid camera movements", *Studies in Computational Intelligence 481* (2013).

[18] Z. Kuś, A. Nawrat, "Object tracking for rapid camera movements in 3D space", *Studies in Computational Intelligence 481* (2013).

[19] A. Nawrat et al., "Design and implementation of innovative unmanned mobile platforms to monitor the state border", Silesian Technical University, Gliwice (2012).

[20] K. Jędrasiak, D. Bereska, A. Nawrat, "The prototype of gyro- stabilized UAV gimbal for day-night surveillance", *Advanced Technologies for Intelligent systems of National Border Security* (2013).